CHANGING SEASONALITY OF CONVECTIVE EVENTS IN THE LABRADOR SEA

A Thesis
Presented to
The Academic Faculty

by

Fan Zhang

In Partial Fulfillment
of the Requirements for the Degree
Master of Science in the
School of Earth and Atmospheric Sciences

Georgia Institute of Technology
May 2014

CHANGING SEASONALITY OF CONVECTIVE EVENTS IN THE LABRADOR SEA

Approved by:

Dr. Annalisa Bracco, Advisor
School of Earth and Atmospheric Sciences
Georgia Institute of Technology

Dr. Taka Ito
School of Earth and Atmospheric Sciences
Georgia Institute of Technology

Dr. Jean Lynch-Stieglitz
School of Earth and Atmospheric Sciences
Georgia Institute of Technology

Date Approved: April 7, 2014

To my mother, Shuxiang Wu,
father, Fenghe Zhang and
little sister, Linyuan Zhang

ACKNOWLEDGEMENTS

I wish to thank my advisor Dr. Bracco and co-advisor Dr. Ito for their guidance and patience in oceanography and in scientific research. Also thanks to Hao and Yisen for their help and suggestions on all aspects.

TABLE OF CONTENTS

LIST OF TABLES

LIST OF FIGURES

SUMMARY

The representation of deep convection in ocean models is a fundamental challenge for climate science. Here a regional simulation of the Labrador Sea circulation and convective activity obtained with the Regional Oceanic Modeling System (ROMS) over the period 1980-2009 is used to characterize the response of convection to atmospheric forcing and the variability in its seasonal cycle. This integration compares well with the sparse in time and space hydrographic surveys and ARGO data (Luo et al. 2012). It is found that convection in the convective region of the Labrador Sea has experienced variability in three key aspects over the 30 years considered. First, the magnitude of convection varies greatly at decadal scales. This aspect is supported by the in-situ observations. Second, the initiation and peak of convection (i.e. initiation and maximum) shift by two to three weeks between strong and weak convective years. Third, the duration of convection varies by approximately one month between strong and weak years. The last two changes are associated to the variability of winter and spring time heat fluxes in the Labrador Sea, while the first results from changes in both atmospheric heat fluxes and oceanic conditions through the inflow of warm Irminger Water from the boundary current system to the basin interior. Changes in heat fluxes over the Labrador Sea convective region are strongly linked to large scale modes of variability, the North Atlantic Oscillation and Arctic Oscillation. Correlations between the mode indices and the local heat fluxes in the convective area are largest in winter during strong, deep events and in spring whenever convection is shallow.

CHAPTER 1

INTRODUCTION

The Meridional Overturning Circulation (MOC) plays a critical role in transporting heat across latitudes in the ocean, and its variability has significant impacts of the global climate system (Bryden et al., 2005). The variability of MOC is largely determined by convection (deep water formation) in several specific regions, including the Nordic Seas and the Labrador Sea (Dickson et al., 1996; Marshall et al., 2001; Marsh et al., 2005; Cunningham and Marsh, 2010), where the ocean releases heat to the atmosphere in winter and the surface waters become dense enough to sink by convective instability (Kuhlbrodt et al. 2007).

In particular, the convection in the Labrador Sea has received much attention, where wintertime deep convection could reach as deep as 2000 m, forms the Labrador Sea Water (LSW) and feeds the MOC (Marshall et al., 1998; Lazier et al., 2002; Rhein et al., 2002). Therefore, the variability of LSW therefore influences the MOC: an intensification of the convective activity in the Labrador Sea will lead to an intensification of the MOC, and consequently to an overall increase in poleward heat transport (Eden and Willebrand 2001).

The formation of LSW displays strong interannual variability influenced by atmospheric fluxes, which are highly variable at high latitudes such as the Labrador Sea, and by the Irminger Current (Myers et al. 2007; Rattan et al. 2010). The Irminger Current is a warm and salty subsurface current that flows along the Greenland coast and is advected through anticyclonic mesoscale eddies into the central Labrador Sea (Lilly et al. 2003; Katsman et al. 2004; Bracco et al. 2008; Hátún et al. 2007; Chanut et al. 2008; Rykova et al. 2009; Gelderloos et al. 2011; Luo et al. 2012). Hence, the variability of the Irminger Current, which has experienced continuous warming since the mid-1990s, is likely to influence the physical conditions in the central Labrador Sea. In fact, hydrographic observations indicate that the convection in the Labrador Sea experienced interannual variability in the past decades (Lazier et al., 2002; Yashayaev, 2007; Yashayaev and Loder, 2009), along with a warming between 1995-2009 (Luo et al., 2012; Yashayaev, 2007).

Such hydrographic surveys has been conducted in the Labrador Sea once a year in late spring or summer by the Bedford Institute of Oceanography (BIO) and Fisheries and Ocean Canada (DFO), and by ARGO profiling floats since June 2002. The surveys primarily sample the AR7W WOCE/CLIVAR line extending from Newfoundland (53.67° N, 55.5° W) to the west coast of Greenland (60.5° N, 48.25° W), and have been extensively used in the literature to investigate the physical conditions of the basin (e.g. Lazier et al. 2002; Yashayaev et al. 2003; Lu et al. 2006; Yashayaev 2007; Yashayaev et al. 2007; Yashayaev and Loder 2009). ARGO floats, on the other hand, provide temperature and salinity measurements of the upper 2000 m, and represent a continuous dataset in time (Yashayaev and Loder 2009; Luo et al. 2012). During 1980-2009, in-situ data show that the convection in the Labrador Sea intensified in the late 1980s and early 1990s, and weakened sensibly since 1995, with a limited recovery in the 2007-2008 winter (Våge et al. 2008; Yashayaev and Loder 2009). Various external causes have been proposed to influence the onset and intensity of convection, including local and remote atmospheric forcing, the Irminger Current conditions, and the state of the subpolar gyre (Marshall and Schott 1999; Lazier et al. 2002; Straneo 2006; Straneo et al. 2010; Luo et al. 2012).

Changes in characteristics of the convective events, other than their intensity, however, have not been investigated, and cannot be investigated using the available observations. Here we use two of the numerical simulations described in Luo et al. 2012 (LBYD12 hereafter) to investigate how the timing and seasonality of convection vary in years of intense versus weak activity. Possible drivers of those changes are explored.

The model configuration is described in Chapter 2 and then validated in Chapter 3. Chapter 4 shows the changes of convection and the results are discussed and Chapter 5 concludes the thesis.

CHAPTER 2

MODEL CONFIGURATION

The Regional Ocean Modeling System (ROMS) is a free-surface, primitive equation model based on the Boussinesq approximation and hydrostatic balance (Shchepetkin and McWilliams, 2003, 2005). Here ROMS is configured in the Labrador Sea over the domain 35-65 ^{o}W, 51-66^{o}N (Fig. 1), with horizontal resolution of 7.5 km and 30 vertical layers, 8 of which are confined in the upper 300 m. The nonlocal K-Profile Parameterization (KPP) scheme is used to parameterize vertical mixing (Large et al., 1994). The integration period begins in January 1980 and ends in December 2009.

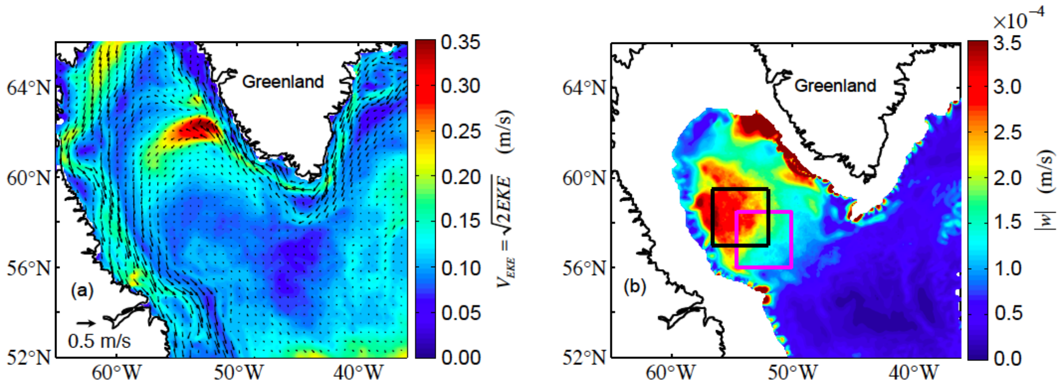

Fig. 1 (a) Annual mean distribution of surface eddy kinetic energy cast as a speed $V_{EKE} = \sqrt{2EKE}$ (in color) and mean surface velocity (arrows). (b) Annual mean distribution of vertical velocity *w* averaged between 150 and 2000 m depth. The magenta box indicates the location of the Central Labrador Sea (CLS) as traditionally defined. The black box indicates the convective regions defined in the paper.

The bathymetry is derived from ETOPO2 (Smith and Sandwell, 1997). A modified Shapiro smoother (Penven et al., 2008) is applied to the original bathymetric data to avoid pressure gradient errors. The smoother is applied everywhere except for three regions around Cape Desolation. Retaining the original bathymetric details only in these regions does not significantly affect the bottom velocities. However, these details are critical for a correct representation of the eddy-generation along the West Greenland coast, as shown by Bracco et al. (2008). A detailed discussion of this problem is contained in Appendix A of Luo et al. (2011).

Boundaries are open to the east, south and north sides of the domain, where the velocity, temperature and salinity fields are nudged to the Simple Ocean Data Assimilation (SODA) ocean reanalysis version 2.1.6 (Carton and Giese, 2008). A modified radiation boundary condition is also applied following Marchesiello et al. (2001). SODA has been evaluated against other ocean reanalysis products in Luo et al. (2013), and it presents the advantage of reproducing quite realistically the lateral and vertical extension of the Irminger Current at the north-east corner of the domain. As mentioned, the time period investigated in this work extends from 1980 to 2009. Since SODA 2.1.6 ends in 2008, boundary conditions of 2008 are repeated for the computation of 2009. Surface fluxes are from NCEP/NCAR (1980-2009). To avoid long-term drift of SST linked to the errors in the NCEP/NCAR fluxes (Josey, 2001), the NCEP/NCAR surface heat fluxes (Q_{NCEP}) are corrected by the NOAA extended SST (SST_{NOAA}) (Smith and Reynolds, 2004) on a monthly timescale and $2^o \times 2^o$ resolution. The heat fluxes forcing the models (Q_{Model}) are calculated as:

$$Q_{Model} = Q_{NCEP} + dQ_{Model}/dSST_{Model} \times (SST_{Model} - SST_{NOAA}).$$

Here we consider two simulations forced by the same atmospheric forcings, consisting of monthly varying NCEP/NCAR heat and momentum fluxes, but by different ocean boundary conditions. In the first simulation (CLIMA), we nudge the open boundaries to monthly mean climatological values obtained averaging the SODA monthly output from 1980 to 2009 (where 2009 is identical to 2008). In the second simulation (VARY), we retain the interannual variability in the boundary conditions and use monthly SODA values without any further averaging. The difference in boundary conditions between CLIMA and VARY ensures that CLIMA removes while VARY retains the interannual variability of the boundary currents.

Initial conditions for both integration are derived from a spin-up run, forced by climatological monthly averaged NCEP/NCAR atmospheric fluxes and SODA boundary conditions, that extend for 50 years after a stationary state is reached. CLIMA and VARY are then initiated in 1976 and the first four years of simulations are discarded.

CHAPTER 3

VALIDATION OF MODEL OUTPUT AND POTENTIAL TEMPERATURE VARIABILITY

A detailed validation of the model representations of the surface circulation in the Central Labrador Sea (CLS) and the interannual variability of potential temperature (PT) throughout the water column are provided respectively in Luo et al. (2011) (LBD11 in the following) and Luo et al. (2012) (LBYD12). The model surface circulation has been compared in detail to TOPEX/Poseidon satellite altimeter data in LBD11. ROMS reproduces accurately the surface circulation and its variability, from seasonal to interannual scales, including the model surface eddy kinetic energy (EKE) along the Greenland coast and in the convective area. Independently of the forcing fields used, and although the horizontal resolution is just below the Rossby radius of deformation (~13 km) in the Labrador Sea the model captures the observed eddy variability. In particular, most statistics related to the mesoscale eddies are in good agreement with the observations, with the exception of the lifespan of those large eddies (six to seven months in CLIMA and eight to eleven months in VARY, on average, versus twelve to eighteen months in the observational records).

The interannual variability of potential temperature in CLS between 0 - 2800 m is discussed in LBYD12. The first half of the record is characterized by the alternation of warmer and colder periods, while the second half is dominated by a warming trend beginning around 1995 in both CLIMA and VARY. Such a trend has been reported by a number of observational studies (e.g. Lazier et al., 2002; Straneo et al., 2010; van Aken et al., 2011; Yashayaev, 2007). For instance, the model successfully captures the strong convection events in 1982-1984 and in the early 1990s', the reduction in the convective activity after 1995 and the partial recovery in 2008. After verifying that the amplitude of the interannual variability of PT compares very well with the available observations, LBYD12 showed that the warming in CLS is the combined result of changes in local heat fluxes and warming of the Irminger Current, which has been reported since 1995 (Böning et al., 2006; Straneo et al., 2010) and is realistically represented in SODA. Irminger Current water is advected by mesoscale eddies to the CLS and increases the restratification (Katsman et al., 2004; Luo et al., 2011).

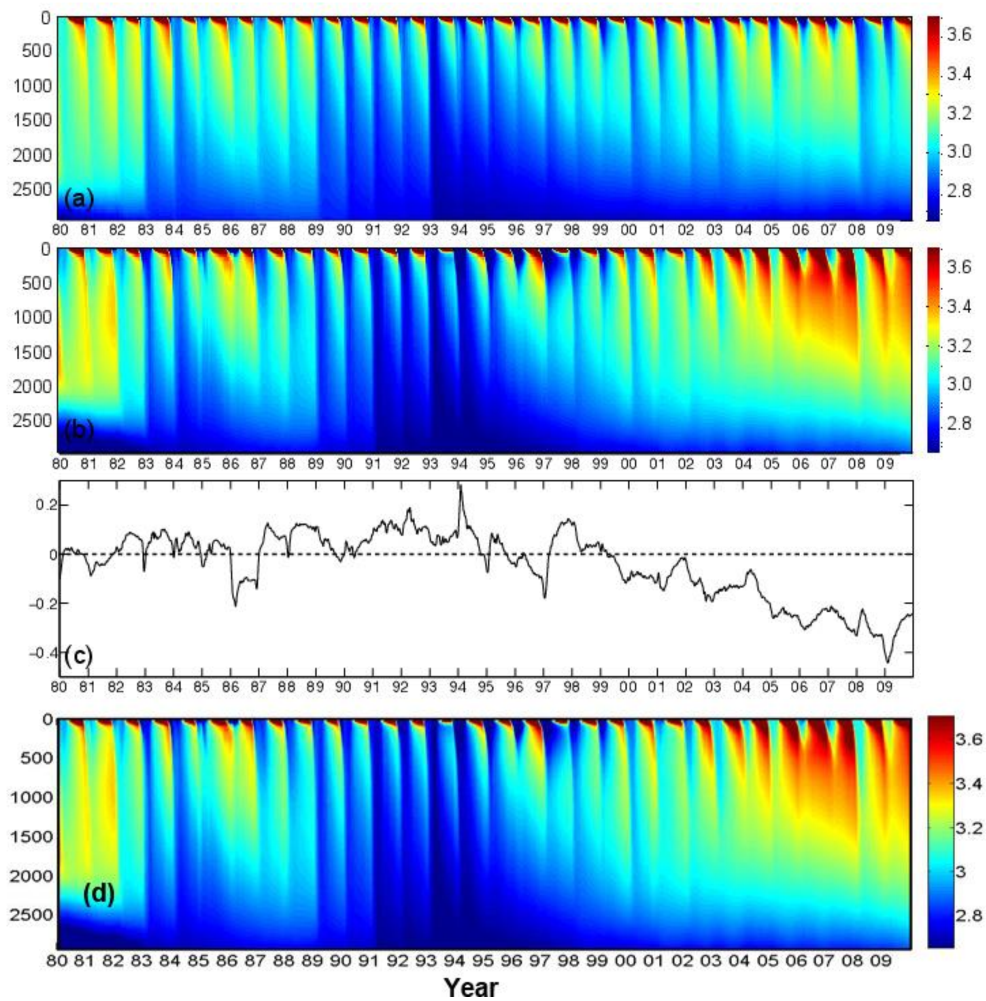

Fig. 2 Evolution of potential temperature from 1980 to 2009. (a) CLIMA in CLS, (b) VARYin CLS, (c) difference between the two integrations (CLIMA-VARY) for potential temperature time series obtained averaging from 150 to 2000 m depth in CLS and (d) VARY in the convective region.

The influence of the Irminger Current warming on the PT in the CLS is quantified by the difference between CLIMA and VARY (Fig. 2c). For the first half of the record the potential temperature averaged between 150 and 2000 m depth over the CLS domain is greater in CLIMA by slightly less than 0.1 ^{o}C on average. After 1995, on the other hand, PT in VARY is consistently higher than in CLIMA by as much as 0.38 ^{o}C at the end of the record (Fig. 2c), and displays a warming trend consistent with the one found in the incoming Irminger Current at the model boundary (see LBYD12, their Fig. 9). As shown in LBYD12, the boundary current contribution explains about half of the CLS warming recorded by VARY after 1995.

It is important to notice that the Irminger Current warming recorded after 1995 is not unprecedented, at least according to SODA, but part of the decadal variability of the system. The period from 1958 to 1970 was indeed characterized by an Irminger Current as warm as during the first decade of the XXI century.

CHAPTER 4

SEASONALITY OF CONVECTIVE EVENTS IN THE LABRADOR SEA

Vertical Velocity and Convection

Fig. 1b shows the annual mean vertical velocity field in the basin as modeled by ROMS. It is clear that CLS does not coincide with the area of maximum convection as measured by the vertical velocity. Such convective region, with larger vertical velocity, is located to the northwest and is better approximated by the black box in Fig. 1b with coordinates (56.6 – 52^{o} W, 57 - 59.5^{o} N). The absolute value of the vertical velocity averaged over the convective region and the whole water column can be used as a proxy to evaluate the strength of convective events (Fig. 3), as high vertical velocities are associated with strong convection, and vice versa shallow events are characterized by limited vertical excursions. The interannual variability of convection over the convective region measured by the vertical velocity field is displayed in Fig. 3. The modeled interannual variations are consistent with hydrographic observations (Lazier et al. 2002; Yashayaev 2007; LBYD12); for example, the model successfully captures the strong convection events in 1983-1983 and in the early 1990s', the reduction in the convective activity after 1995 and the partial recovery in 2008.

Independently of the integration considered, the intensity of convection in the convective region is reduced significantly after 1995 in both CLIMA and VARY. The averaged vertical velocity is about 1.5×10^{-3} m/s in 1980-1994 and decreases to approximately 0.7×10^{-3} m/s after 1995.

Although the vertical velocities in the convective region in CLIMA and VARY display identical seasonal cycle and similar interannual variability (Figs. 3 and 4), they differ slightly in their intensity, due to the interannual changes in the Irminger Current temperature that impact convection. Due to the boundary current warming recorded from 1995 to 2007-2008, both the CLS and the convective region in VARY is subjected to an increased restratification through the advection of warmer and more saline water through lateral mixing by Irminger Rings.

In the following we separately consider years of deep and shallow convection using the vertical velocity averaged over the CR region and over 150 and 2000 m depth. Deep convection years are defined as those when the absolute strength of the vertical velocity field in VARY exceeds 0.55×10^{-3} m/s. Such a threshold, although it does not correspond to the commonly accepted one of mixed-layer depth exceeding 1000 m (e.g. Pickart et al., 2003), provides a similar differentiation, and allows us to group 15 years (1980, 1982, 1983, 1984, 1988, 1989, 1990, 1991, 1992, 1993, 1994, 1995, 1999, 2000, 2008) and 15 years (1981, 1985, 1986, 1987, 1996, 1997, 1998, 2001, 2002, 2003, 2004, 2005, 2006, 2007, 2009) in the deep and shallow convection categories, respectively

Seasonality and Strength of Convection

The seasonal cycle of convective events over the Labrador Sea can be quantified in the observations only using Argo data from mid-2002 onward, as shipboard and hydrographic surveys are usually limited to late spring and summer. The Argo period, however, is strongly biased, being characterized by all but one (2008) shallow convective episodes. Given that ROMS reproduces well both the observed seasonal cycle from mid-2002 and the interannual variability of the observed potential temperature in the CLS (LBYD12), we can safely assume that it provides a good representation of seasonal changes at all times.

Overall shallow and deep (or weak and strong) convective events differ in the time of their initiation, maxima and shutdown (Fig. 4a). Weak events initiate two to three weeks after the strong ones, they reach their peak of intensity two weeks later, and display a two-week shorter duration. Such a behavior is common to all weak events, independently of the decade considered. Consequently, the convective activity in weak years is approximately one month shorter than in strong ones and shifted further into spring.

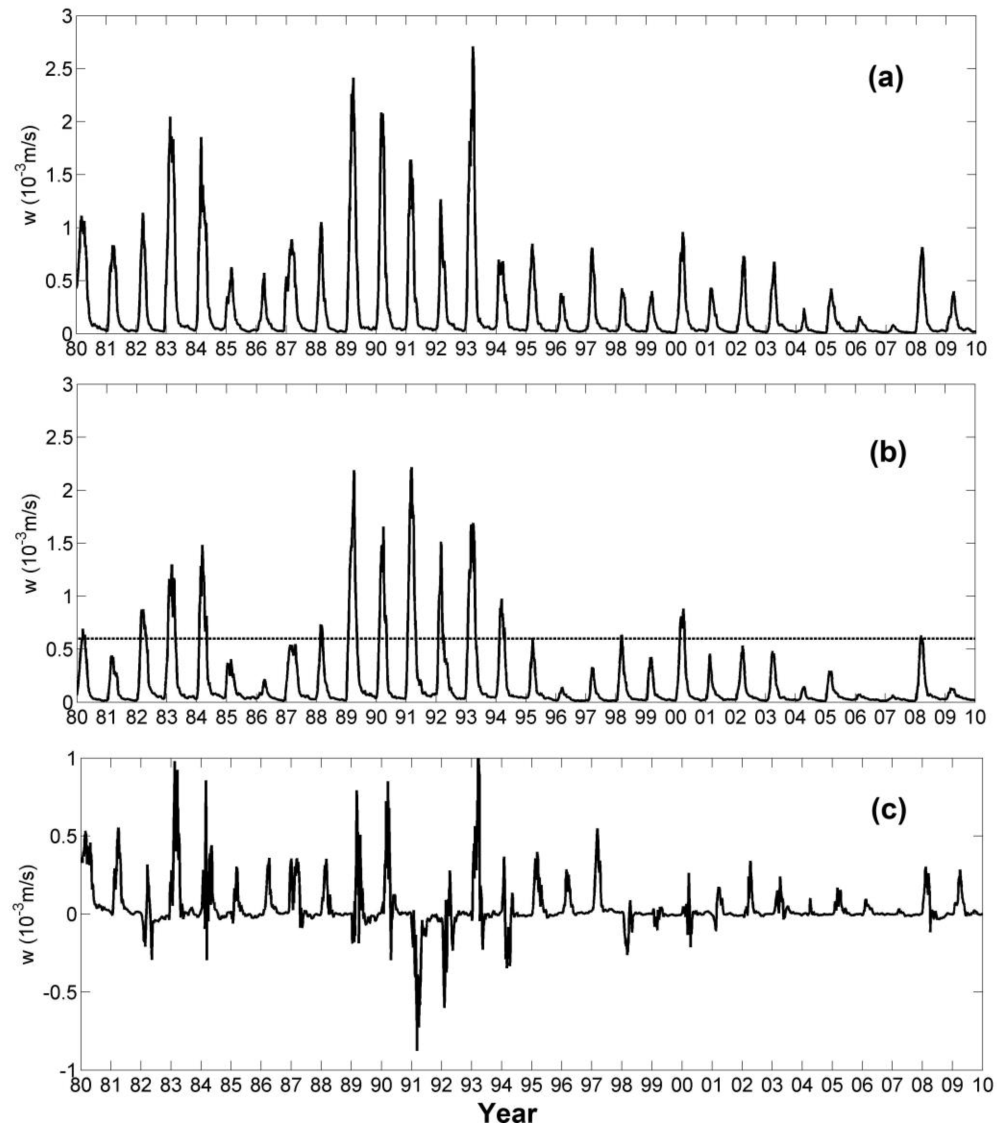

Fig. 3 Time series of vertical velocity averaged over the convective region between 150 and 2000 m depth from 1980 to 2009. (a) CLIMA, (b) VARY and (c) the difference (CLIMA-VARY). Unit: 10^{-3} m/s. The dashed line in (b) indicates the chosen threshold separating strong and weak convections years.

The reduced intensity, shifted seasonality and shortened duration of convection in the convective region in years of shallow convection in both integrations is explained by accompanying reduced heat fluxes and wind intensity in winter (Figs. 4c and 4d). It is noticeable that atmospheric changes are found only between November and March, while both heat and momentum fluxes do not show any significant difference through the remaining of the year. The atmospheric fluxes display a change in intensity, but no shift of seasonality is found in their annual cycle.

Since the convective region loses heat to the atmosphere in winter and the surface waters cool and eventually become dense enough to sink, the two-week delay of convection initiation could be explained as: because of the reduced heat flux and wind intensity, it takes two weeks more for the convection to start.

Another important factor influencing the convection in the convective region is the input of warm, salty Irminger water from Western Greenland coast mediated by the mesoscale eddies. Those large eddies increase the stratification in the convective region through lateral mixing (Lilly et al., 2003; Katsman et al., 2004; Chanut et al., 2008; Gelderloos et al., 2011; LBYD12). The increased stratification requires the convective region to release more heat to the atmosphere to induce convection, further delaying its initiation. The impact of the boundary current interannual variability on convection is quantified as the difference between VARY and CLIMA and it is more prominent in weak than in strong years, due to the significant warming of Irminger Current experienced since 1995 (Myers et al., 2007; Stein, 2005), and therefore co-occurring with most weak years. For instance, the seasonality of convection in VARY is further shifted compared to CLIMA in 1995-2009 and the intensity of convection is reduced from 0.7×10^{-3} m/s to 0.5×10^{-3} m/s (Fig. 4a). In contrast, average vertical velocity in VARY and CLIMA are almost identical in 1980-1994.

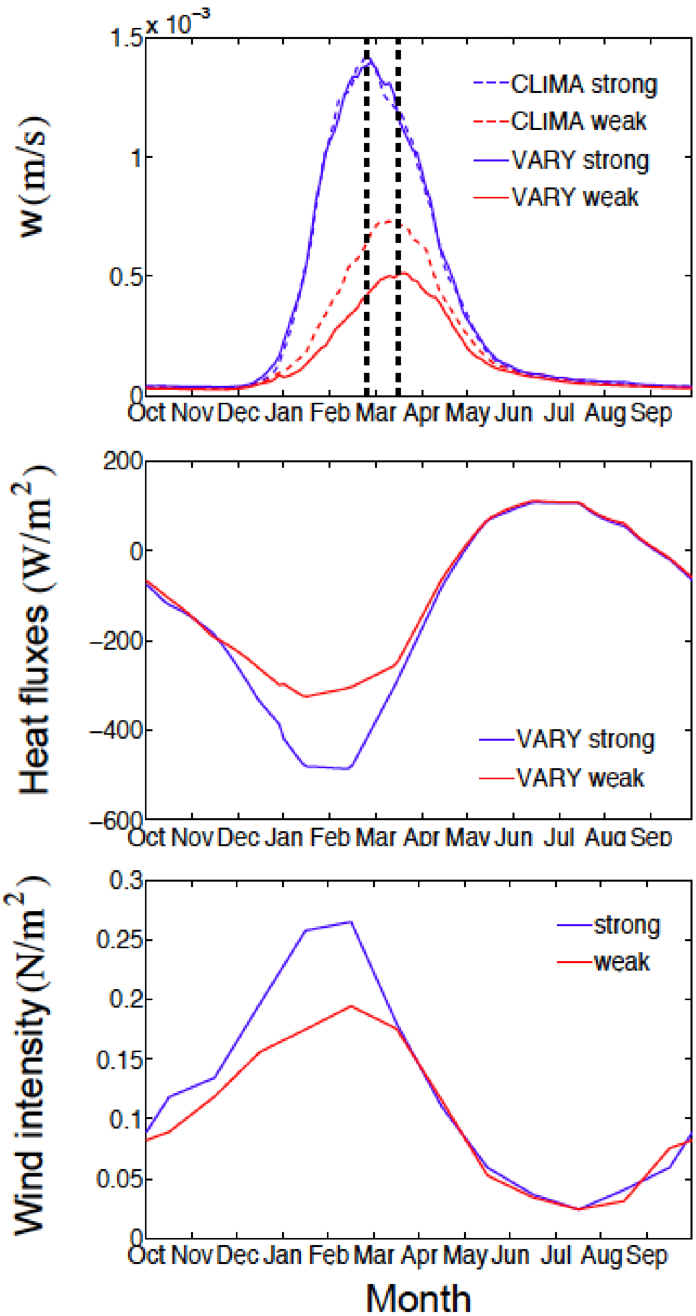

Fig. 4 (a) Annual cycle of vertical velocity averaged between 150 m and 2000 m depth (dashed lines for CLIMA, and solid lines for VARY), (b) of downward surface heat flux Q_{Mod} and (c) surface wind intensity averaged over in the convective region. Dashed lines in (a) indicate the locations when the vertical velocity reaches its maximum.

Strength of Convection and Heat Fluxes

Figure 5 displays the correlation between the strength of convection, measured by the absolute vertical velocity, and heat fluxes averaged over the convective region in different seasons. A strong correlation implies that the convection intensity is regulated by the local heat fluxes. Since convection occur in winter and spring (from January to April; Fig. 4a), the correlation between the convection and the winter-spring heat flux (from December to May) could be as high as 0.93 (Figs. 5a and 5b). A close-up of correlation in winter and spring separately reveals that the wintertime heat flux is more important (Figs. 5c-5f) since it preconditions the ocean to initiate convection. Moreover, the accumulated heat flux in winter is larger than in spring (Fig. 4c).

However, no significant correlation between the convection and the heat flux averaged in previous spring, summer and fall (not shown), implying that the intensity of convection is largely determined by the local atmospheric forcing when it occurs and has little memory of atmospheric forcing from previous seasons.

The strength of convection is also regulated by the inflow of Irminger Current: in VARY correlations are all slightly smaller than in CLIMA, particularly in the winter season, and the slopes describing the linear relation between vertical velocities and heat fluxes change more dramatically between strong and weak years (Fig. 5). Notwithstanding the modulation at decadal scales associated with changes of the Irminger Current, the seasonal variability of the convective activity in the Labrador Sea appears controlled by the local heat fluxes during or immediately preceding the convective season. Heat fluxes over the convective region result from large scale anomalies and are highly correlated with both the North Atlantic Oscillation (NAO) (Dickson et al., 1996), and the Arctic Oscillation (AO) (Thompson and Wallace, 1998) indices (Table 1). In years of strong convection correlations between the local heat fluxes and the AO/NAO indices are higher in winter, while during shallow convection events reach 0.6 for the spring season.

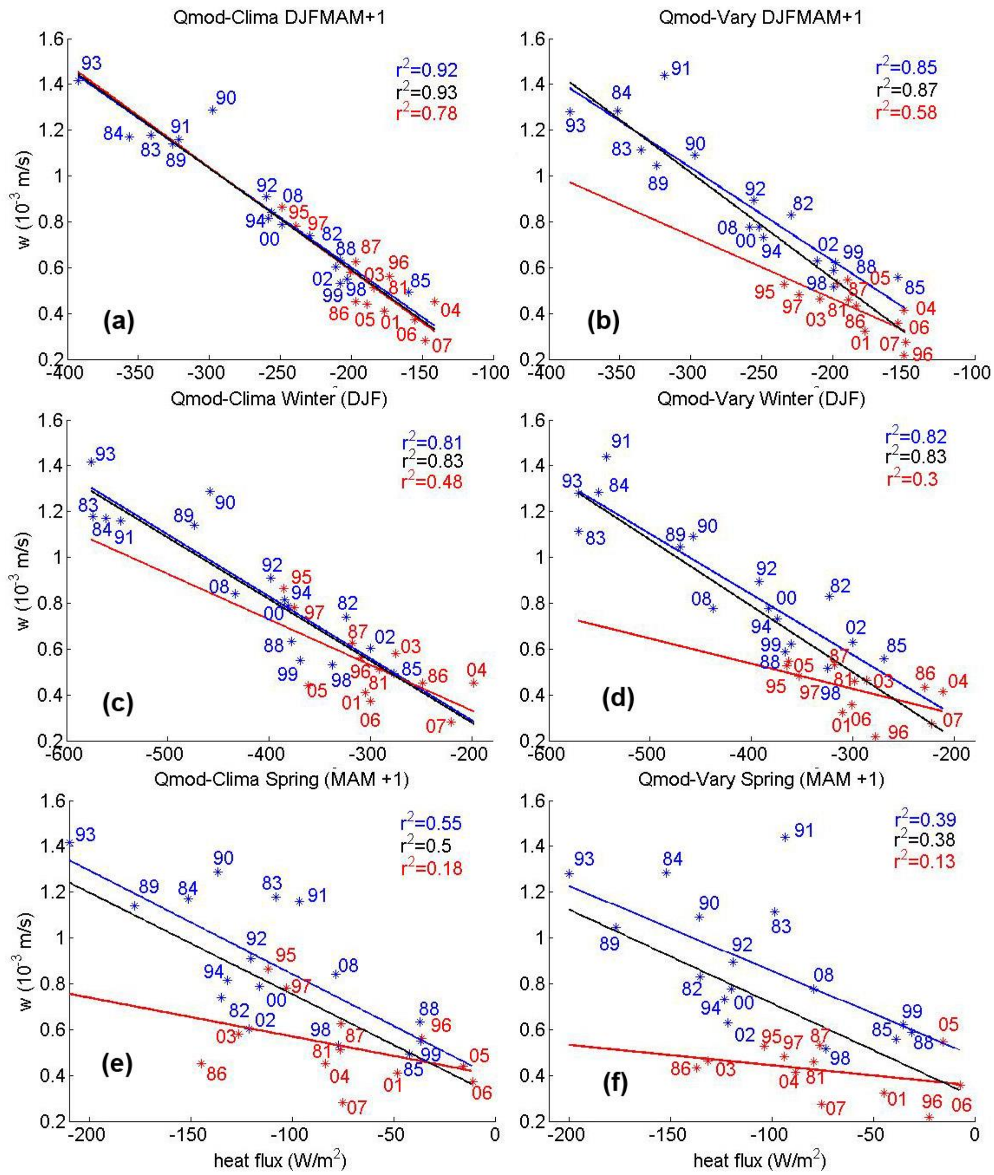

Fig. 5 Relation between downward heat flux as seen by the model (Q_{Mod}) and vertical velocities averaged over the convective region between 150 and 2000 m. An almost identical figure can be obtained using NCEP fluxes. Differences between Q_{NCEP} and Q_{Mod} are very small. (a) CLIMA, winter and spring (December to May, DJFMAM); (b) VARY, DJFMAM; (c) CLIMA winter only, DJF; (d) VARY, DJF; (e) CLIMA spring only, MAM; and (f) VARY, MAM. Blue, red and black lines show fits using strong, weak, and all years, respectively. The two-digit numbers indicate the year.

Table 1: Correlation coefficients between seasonal (DJF, MAM, and DJFMAM) averages of the heat fluxes over the convective region and the AO/NAO indices for 15 strong convective years, 15 weak episodes, and all 30 years. Correlations using monthly values over the same seasons are statistically indistinguishable.

	AO strong	AO weak	AO all	NAO strong	NAO weak	NAO all
Winter (DJF)	0.53	0.32	0.64	0.59	0.30	0.64
Spring+1 (MAM)	0.32	0.59	0.42	0.42	0.63	0.52
WinterSpring+1 (DJFMAM)	0.50	0.26	0.57	0.50	0.26	0.55

The strength of convection depends also by the inflow of Irminger Current waters, as already noticed: in VARY correlations are all slightly smaller than in CLIMA, particularly in the winter season, and the slopes describing the linear relation between vertical velocities and heat fluxes change more dramatically between strong and weak years. Notwithstanding the modulation at decadal scales associated with changes of the Irminger Current characteristics, the seasonal variability of the convective activity in the Labrador Sea appears controlled by the local heat fluxes during or immediately preceding the convective season. Heat fluxes over the CR result from large scale anomalies and are highly correlated with both the North Atlantic Oscillation (NAO) (Dickson et al., 1996), and the Arctic Oscillation (AO) (Thompson and Wallace, 1998) indices (Table 1). In years of strong convection correlations between the local heat fluxes and the AO/NAO indices are higher in winter, while during shallow convection events reach c.c.=0.6 for the spring season.

CHAPTER 5

DISCUSSIONS AND CONCLUSIONS

In this paper, we employ ROMS to investigate the changes of convection in the central Labrador Sea during 1980-2009 in terms of vertical velocity. Two simulations, CLIMA and VARY, are run to isolate the impacts of warming boundary currents on the interannual variability of convection. Both CLIMA and VARY produce realistic circulation, potential temperature and eddy kinetic energy, while results from VARY are more realistic and more close to satellite and hydrographic observations than CLIMA by accounting for the interannual variability of the Irminger Current (Luo et al., 2013).

We find that the reduced intensity, shifted seasonality and shortened duration of convection in the Labrador Sea is largely determined by the reduced local atmospheric forcing, consistent with previous studies (Bentsen et al., 2004; Delworth and Greatbatch, 2000; Eden and Willebrand, 2001). Heat fluxes over the convective region from December to May correlate highly with the oceanic vertical velocities averaged between 150 and 2000 m depth in both simulations, with the wintertime heat flux having larger impacts in years of strong convection (Dickson et al. 1996), and spring heat fluxes being fundamental during weak convective episodes. In contrast, the atmospheric forcings from previous spring, summer and fall do not correlate with the convection well, implying that the convection in the Labrador Sea has little memory of atmospheric forcings from previous conditions.

In addition to the local atmospheric forcing, the boundary current from the Western Greenland coast also contributes to the reduced intensity and shifted seasonality of the convection, as manifested by the difference of vertical velocity between CLIAM and VARY (Fig. 3c). A number of studies suggest that the eddies generated along the Western Greenland coast carry the warm and salty water, propagate southward, and eventually reach CLS and the convective region, increasing the stratification through lateral mixing (Bracco et al., 2008; Katsman et al., 2004; Luo et al., 2011; Straneo, 2006). More quantitatively, comparison between CLIMA and VARY indicates that the boundary current is responsible for about 20% reduction of convection in the convective region (Fig. 4a).

Here we show that shallow and deep convective events are characterized not only by intensity, but also by the seasonal cycle. Both initiation and maximum of convection for weak events in VARY are delayed by about three weeks compared to strong ones. Additionally, the duration of convective activity is approximately one month shorter for shallow episodes. Those characteristics are linked to the reduced atmospheric cooling observed between December and May in the climatology of the heat fluxes during weak years. The seasonal cycle of the atmospheric heat and momentum fluxes is unaltered, but variations in surface cooling rates are translated in changes in intensity, seasonality and duration of ocean convection. Those changes are important for understanding the variability in the oxygen drawdown and carbon sequestration in the basin.

Local heat fluxes reflect atmospheric variability at broader scales, and are highly correlated with NAO/AO in winter during strong events, and in spring for weak years. The high correlation found between the intensity of convective activity in the Labrador Sea and both local and large scale atmospheric heat flux may provide an important test for validating coupled climate models, while pointing to a simple way to parameterize and improve the representation of convection in the basin in coarse resolution models.

REFERENCES

Bentsen, M., H. Drange, T. Furevik, and T. Zhou, 2004: Simulated variability of the Atlantic meridional overturning circulation. Clim. Dyn., 22, 701-720.

Böning, C. W., M. Scheinert, J. Dengg, A. Biastoch, and A. Funk, 2006: Decadal variability of subpolar gyre transport and its reverberation in the North Atlantic overturning. Geophys. Res. Lett., 33, L21S01.

Bracco, A., J. Pedlosky, and R. S. Pickart, 2008: Eddy formation near the west coast of Greenland. J. Phys. Oceanogr., 38, 1992-2002.

Bryden, H. L., H. R. Longworth, and S. A. Cunningham, 2005: Slowing of the Atlantic meridional overturning circulation at 25^{o} N. Nature, 438, 655-657.

Carton, J. A., and B. S. Giese, 2008: A reanalysis of ocean climate using Simple Ocean Data Assimilation (SODA). Mon. Weather Rev., 136, 2999-3017.

Chanut, J., B. Barnier, W. Large, L. Debreu, T. Penduff, J. M. Molines, and P. Mathiot, 2008: Mesoscale eddies in the Labrador Sea and their contribution to convection and restratification. J. Phys. Oceanogr., 38, 1617-1643.

Delworth, T. L., and R. J. Greatbatch, 2000: Multidecadal thermohaline circulation variability driven by atmospheric surface flux forcing. J. Clim., 13, 1481-1495.

Dickson, R., J. Lazier, J. Meincke, P. Rhines, and J. Swift, 1996: Long-term coordinated changes in the convective activity of the North Atlantic. Prog. Oceanogr., 38, 241-295.

Eden, C., and J. Willebrand, 2001: Mechanism of interannual to decadal variability of the North Atlantic circulation. J. Clim., 14, 2266-2280.

Gelderloos, R., C. A. Katsman, and S. S. Drijfhout, 2011: Assessing the roles of three eddy types in restratifying the Labrador Sea after deep convection. J. Phys. Oceanogr., 41, 2102-2119.

Häkkinen, S., and P. B. Rhines, 2004: Decline of subpolar North Atlantic circulation during the 1990s. Science, 304, 555-559.

Holland, D. M., R. H. Thomas, B. De Young, M. H. Ribergaard, and B. Lyberth, 2008: Acceleration of Jakobshavn Isbrae triggered by warm subsurface ocean waters. Nat. Geosci., 1, 659-664.

Josey, S., 2001: A comparison of ECMWF, NCEP-NCAR, and SOC surface heat fluxes with moored buoy measurements in the subduction region of the northeast Atlantic. J. Clim., 14, 1780-1789.

Katsman, C. A., M. A. Spall, and R. S. Pickart, 2004: Boundary current eddies and their role in the restratification of the Labrador Sea*. J. Phys. Oceanogr., 34, 1967-1983.

Kuhlbrodt, T., A. Griesel, M. Montoya, A. Levermann, M. Hofmann, and S. Rahmstorf, 2007: On the driving processes of the Atlantic meridional overturning circulation. Rev. Geophys., 45, RG2001.

Large, W. G., J. C. McWilliams, and S. C. Doney, 1994: Oceanic vertical mixing: A review and a model with a nonlocal boundary layer parameterization. Rev. Geophys., 32, 363-403.

Lazier, J. R. N., R. Hendry, A. Clarke, I. Yashayaev, and P. Rhines, 2002: Convection and restratification in the Labrador Sea, 1990–2000. Deep Sea Res. Part I, 49, 1819-1835.

Lilly, J. M., P. B. Rhines, F. Schott, K. Lavender, J. Lazier, U. Send, and E. D'Asaro, 2003: Observations of the Labrador Sea eddy field. Prog. Oceanogr., 59, 75-176.

Lu, Y., D. G. Wright, and I. Yashayaev, 2007: Modelling hydrographic changes in the Labrador sea over the past five decades, Prog. Oceanogr., 73, 406-426.

Luo, H., A. Bracco, and E. Di Lorenzo, 2011: The interannual variability of the surface eddy kinetic energy in the Labrador Sea. Prog. Oceanogr., 91, 295-311.

Luo, H., A. Bracco, I. Yashayaev, and E. Di Lorenzo, 2012: The interannual variability of potential temperature in the central Labrador Sea. J. Geophys. Res., 117, C10016, doi:10.1029/2012JC007988.

Marchesiello, P., J. C. McWilliams, and A. Shchepetkin, 2001: Open boundary conditions for long-term integration of regional oceanic models. Ocean Model., 3, 1-20.

Marshall, J., and Coauthors, 1998: The Labrador Sea deep convection experiment. Bull. Am. Meteorol. Soc., 79, 2033-2058.

Marshall, J., and F. Schott, 1999: Open-ocean convection: Observations, theory, and models. Rev. Geophys, 37, 1-64.

Marshall, J., and Coauthors, 2001: North Atlantic climate variability: phenomena, impacts and mechanisms. Int. J. Climatol., 21, 1863-1898.

Myers, P. G., N. Kulan, and M. H. Ribergaard, 2007: Irminger water variability in the West Greenland Current. Geophys. Res. Lett., 34, L17601.

Penven, P., P. Marchesiello, L. Debreu, and J. Lefèvre, 2008: Software tools for pre-and postprocessing of oceanic regional simulations. Environ. Model. Software, 23, 660-662.

Pickart, R. S., M. A. Spall, M. H. Ribergaard, G. K. Moore, and R. F. Milliff, 2003: Deep convection in the Irminger Sea forced by the Greenland tip jet. Nature, 424, 152-156.

Rattan, S., P. G. Myers, A.-M. Treguier, S. Theetten, A. Biastoch, and C. Böning, 2010: Towards an understanding of Labrador Sea salinity drift in eddy-permitting simulations, Ocean Model., 35, 77-88, doi:10.1016/j.ocemod.2010.06.007.

Rhein, M., and Coauthors, 2002: Labrador Sea Water: Pathways, CFC inventory, and formation rates. J. Phys. Oceanogr., 32, 648-665.

Rykova, T., F. Straneo, J. M. Lilly, and I. Yashayaev, 2009: Irminger current anticyclones in the Labrador Sea observed in the hydrographic record, 1990-2004, J. Mar. Res., 67, 361-384.

Shchepetkin, A. F., and J. C. McWilliams, 2003: A method for computing horizontal pressuregradient force in an oceanic model with a nonaligned vertical coordinate. J. Geophys. Res., 108, 3090.

——, 2005: The regional oceanic modeling system (ROMS): a split-explicit, free-surface, topography-following-coordinate oceanic model. Ocean Model., 9, 347-404.

Smith, T. M., and R. W. Reynolds, 2004: Improved extended reconstruction of SST (1854-1997). J. Clim., 17, 2466-2477.

Smith, W. H., and D. Sandwell, 1997: Marine gravity anomaly from Geosat and ERS 1 satellite altimetry. J. Geophys. Res., 102, 10039-10054.

Stein, M., 2005: North Atlantic subpolar gyre warming–impacts on Greenland offshore waters. J. Northw. Atl. Fish. Sci., 36, 43-54.

Straneo, F., 2006: Heat and freshwater transport through the central Labrador Sea, J. Phys. Oceanogr., 36, 606-628.

Straneo, F., and Coauthors, 2010: Rapid circulation of warm subtropical waters in a major glacial fjord in East Greenland. Nat. Geosci., 3, 182-186.

Talley, L. D., and M. S. McCartney, 1982: Distribution and circulation of Labrador Sea water. J. Phys. Oceanogr., 12, 1189-1205.

Thompson, D. W., and J. M. Wallace, 1998: The Arctic Oscillation signature in the wintertime geopotential height and temperature fields, Geophys. Res. Lett., 25, 1297-1300.

Våge, K., and Coauthors, 2008: Surprising return of deep convection to the subpolar North Atlantic Ocean in winter 2007–2008. Nat. Geosci., 2, 67-72.

van Aken, H. M., M. Femke de Jong, and I. Yashayaev, 2011: Decadal and multi-decadal variability of Labrador Sea Water in the north-western North Atlantic Ocean derived from tracer distributions: Heat budget, ventilation, and advection. Deep Sea Res. Part I, 58, 505-523.

Yashayaev, I., J. R. N. Lazier, and R. A. Clarke, 2003: Temperature and salinity in the central Labrador Sea, ICES Marine Symposia Series, 219, 32-39.

Yashayaev, I., 2007: Hydrographic changes in the Labrador Sea, 1960–2005. Prog. Oceanogr., 73, 242-276.

Yashayaev, I., H. M. van Aken, N. P. Holliday, and M. Bersch, 2007: Transformation of the Labrador Sea Water in the subpolar North Atlantic, Geophys. Res. Lett., 34, L22605, doi:10.1029/2007GL031812.

Yashayaev, I., and J. W. Loder, 2009: Enhanced production of Labrador Sea Water in 2008, Geophys. Res. Lett., 36, L01606, doi: 10.1029/2008GL036162.